IOPscience iopscience.iop.org

Home Search Collections Journals About Contact us My IOPscience

Areal changes of land ecosystems in the Alaskan Yukon River Basin from 1984 to 2008

This article has been downloaded from IOPscience. Please scroll down to see the full text article.

2011 Environ. Res. Lett. 6 034012

(http://iopscience.iop.org/1748-9326/6/3/034012)

View the table of contents for this issue, or go to the journal homepage for more

Download details:
IP Address: 128.210.127.177
The article was downloaded on 29/08/2011 at 20:29

Please note that terms and conditions apply.

Environ. Res. Lett. **6** (2011) 034012 (9pp) doi:10.1088/1748-9326/6/3/034012

Areal changes of land ecosystems in the Alaskan Yukon River Basin from 1984 to 2008

Xiaoliang Lu and Qianlai Zhuang

Departments of Earth and Atmospheric Sciences and Agronomy, Purdue University, West Lafayette, IN 47907, USA

Received 11 February 2011
Accepted for publication 14 July 2011
Published 29 July 2011
Online at stacks.iop.org/ERL/6/034012

Abstract

Multivariate alteration detection (MAD) and Bayesian inference (BI) methods are used to analyze land cover changes with Landsat images for the Alaskan Yukon River Basin from 1984 to 2008. The US Geological Survey National Land Cover Database 2001 (NLCD 2001) is treated as reference information to detect the changes. It is found that the regional land cover change has three general trends with various potential causes during the study period: (1) forests decreased mainly due to wildfire, (2) the closed water bodies were shrinking possibly due to permafrost degradation if water drains well in discontinuous permafrost regions, (3) shrubs had expanded and a large portion of grassland was converted into shrubland likely due to forest fire and warming. The uncertainty of this analysis may mainly arise from image acquisition date differences and illumination angles and remaining cloud contamination to the images. This study provides a method to analyze land cover changes with Landsat data for other regions. The developed land cover data should help future understanding of permafrost dynamics, biogeochemistry, hydrology and regional climate in the region.

Keywords: remote sensing, land cover change

S Online supplementary data available from stacks.iop.org/ERL/6/034012/mmedia

1. Introduction

Global surface temperature has increased at a rate of 0.13 ± 0.03 °C/decade for the past 50 years [1]. This warming trend is more evident in high northern latitudes [2]. In particular, the climate in Alaska switched its state abruptly from cool and moist to hot and dry in the summer of 1976 while no statistically significant change in annual precipitation was reported from 1951 to 2001 [3]. This warm and dry shift in the climate regime potentially altered land cover [4–6] including the shrinkage of wetlands, drying and succeeding to upland habitat [7], changing of water bodies [8–10] and expanding of shrubs [11, 12] in the region.

Analysis of land cover changes is important for evaluating the transition of ecosystems, the carbon cycle and the water and energy balance in response to climate changes in the sub-arctic region. The change of water bodies and associated wetland areas will in turn affect the carbon balance, including methane dynamics in the sub-arctic [13, 14]. To date, there is a lack of studies examining land cover changes in a high spatial resolution manner in the sub-arctic. Satellite sensors with a 1 km or coarser resolution are not suitable for detecting the dynamics of relatively small water bodies and new sensors with finer resolutions lack long-time records. In contrast, the Landsat satellites provide a longer temporal record of land observations and Landsat data have been used to reconstruct the history of the Earth's land surface back to 1972 for various regions [15].

The Yukon River Basin is the fourth largest basin in North America with a drainage area of 832 700 km^2, of which 508 900 km^2 is in Alaska (figure 1). It has large variations in topography: low rolling hills and low mountains account for 61% of the total area, plains and lowlands account for 20% and around 19% is occupied by high rugged mountains. The region has permafrost underneath, which can be categorized into five types [16]: continuous permafrost with high, medium and low

 © 2011 IOP Publishing Ltd Printed in the UK

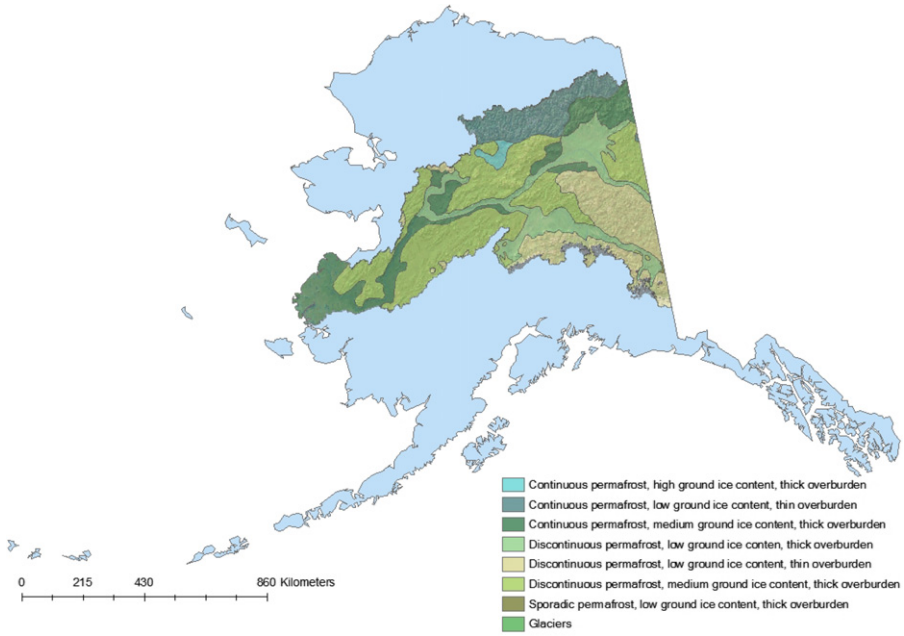

Figure 1. The Yukon River Basin in Alaska and the distribution of permafrost and ground ice conditions [14].

ice content, each accounting for 1.2%, 17.2% and 11.6% of the permafrost area, respectively, and discontinuous permafrost with medium and low ice content accounting for 36.3% and 33.6% of the permafrost area, respectively. The analysis of land cover change in the region will help our understanding of the carbon and water cycling. However, to date, there is a lack of efforts to analyze the land cover change in the region. Here we take advantage of the available Landsat images to investigate the land cover change in the Alaskan Yukon River Basin from 1984 to 2008. We further explore the possible causes for the identified changes.

2. Methods

2.1. Overview

We first obtained Landsat images from 1984 to 2008 and National Land Cover Database 2001 (NLCD 2001) data for the region [17]. Second, we removed the effects of terrain, cloud and associated shadow from the Landsat images. Third, we used the multivariate alteration detection (MAD) [18–20] and a Bayesian inference (BI) method [21] to identify the areal change using the NLCD 2001 data as reference. Fourth, we corrected the possible classification biases using the probabilistic label relaxation (PLR) method [22]. Finally, we analyzed the potential causes for the areal changes of major land cover types. More detailed method information is provided as supplementary material (see figure S1 available at stacks.iop.org/ERL/6/034012/mmedia for the overall flowchart of the land cover mapping method).

2.2. Satellite data acquisition and pre-processing

Landsat TM and ETM+ images for the four periods of 1984–9, 1990–5, 1996–2001 and 2003–8 in the Yukon River Basin were obtained (http://glovis.usgs.gov). Each period consisted of 26–31 scenes and all images were selected for the period between 15 June and 30 August to minimize errors due to seasonal and annual phenological cycles (see the supplementary material for the data used, available at stacks.iop.org/ERL/6/034012/mmedia). Each period consisted of 26–31 scenes (total of 155) selected for peak vegetation cover and minimal cloud cover to minimize errors due to seasonal and annual phenological cycles. Two thirds of the scenes were between 15 June and 30 August, with the dates of the additional 52 scenes ranging from 16 May to 24 September. The cloud cover category was 0% for most scenes, with 12 scenes with 1–9% cloud cover, 14 scenes with 10% and 4 scenes with 20%. The images acquired during or near significant rainfall events were excluded based on meteorological precipitation data [23].

The automatic cloud cover assessment (ACCA) algorithm was used to detect clouds over the images [25]. Further, a combination of geometric and optical constraints was used to detect cloud shadows [26]. Specifically, we estimated the position of the cloud shadow from shadow length and direction. We acquired the cloud shadow length for each scene and determined the direction of the cloud shadows based on the solar azimuth angle. Next we used the semi-empirical cosine correction (C-correction) method to correct the images for the effects of local solar illumination [27]. The required digital elevation model (DEM) for processing the Landsat data was extracted from the Global, 1 arc second (approximately 30 m) digital elevation model (GDEM) [24].

2.3. Change detection and classification

With the corrected Landsat data, the land cover change for periods other than 2001–3 was detected based on NLCD 2001 data [17]. In this study, images acquired during 2001–3 were used as reference image and it was assumed they have the same land cover distribution as NLCD 2001. Using the MAD method, a pair of two images at a given time was spectrally

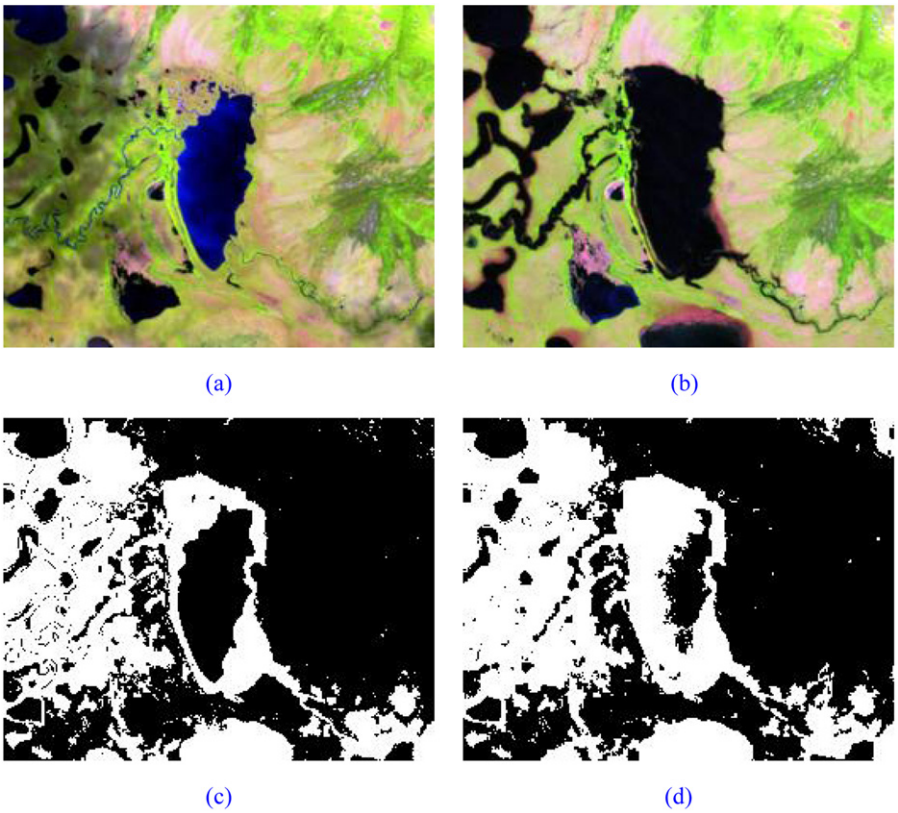

Figure 2. Effects of MAD component selection on the final change detection: (a) and (b) are the Landsat ETM+ color composite scenes of band5 (red), band4 (green) and band3 (blue) acquired over a lake in the Yukon River Basin in August 1999 and July 2001, respectively; (c) and (d) are the change detection results derived from the first MAD component (MAD1) and the first two components (MAD1 and MAD2), respectively. Black color stands for no change and white color indicates the changed areas.

compared. One was the reference image during the period of 2001–3 and the other image was to be analyzed with respect to land cover changes. First, all raw digital number (DN) records of these images were converted into top-of-atmosphere (TOA) reflectance data [28]. The six spectral channels (without the thermal band) in the two images were then linearly transformed into two variates whose transformation coefficients were determined by minimizing the positive correlation between the two variates. The change detection analysis was then applied to the difference between two MAD variates. Note that the bias due to the sensors or atmospheric factors was also minimized in the transformation, thus the difference between the two MAD variates only provided the information on the land cover change between the two images. For example, the Landsat ETM+ color composite scenes of band5 (red), band4 (green) and band3 (blue) acquired over a lake in the Yukon River Basin in August 1999 and July 2001, respectively were analyzed (figure 2). The detection results were derived from the first MAD component (MAD1) and the first two components MAD1 and MAD2, respectively. Here we only used MAD1 in our analysis. The difference between the two MAD variates was approximated using three Gaussian components that correspond to negative change, no change and positive change, respectively. If there is no change, the MAD variates are near zero. Negative and positive values of MAD variates indicate changes. The BI method was used to determine if there was a change in MAD variates. Detailed information on the MAD and BI methods is provided in the supplementary material (available at stacks.iop.org/ERL/6/034012/mmedia).

Next, we randomly selected 25 000 no-change pixels to train classifiers for land cover types for each scene. We combined the NLCD classification system into eight classes as the final results (see the supplementary material for the combination rule, available at stacks.iop.org/ERL/6/034012/mmedia). Due to the linear treatment of the atmospheric effect and the resulting uncertainties in the transformation coefficients and the use of the pixel-oriented classifier, there was some 'salt-and-pepper' appearance in the resulting thematic map. The PLR method [22] was then used to improve the spatial coherence. To reduce the effect of flood and the seasonal change of river channels, we delineated streams that were longer than 1 km in the Yukon River Basin based on the National Hydrograph Dataset (NHD, http://nhd.usgs.gov/). The areas within a distance of 150 m from the streams were ignored.

3. Results and discussion

The land cover maps for the periods 1984–9 and 2003–8 and corresponding change detection results are shown in

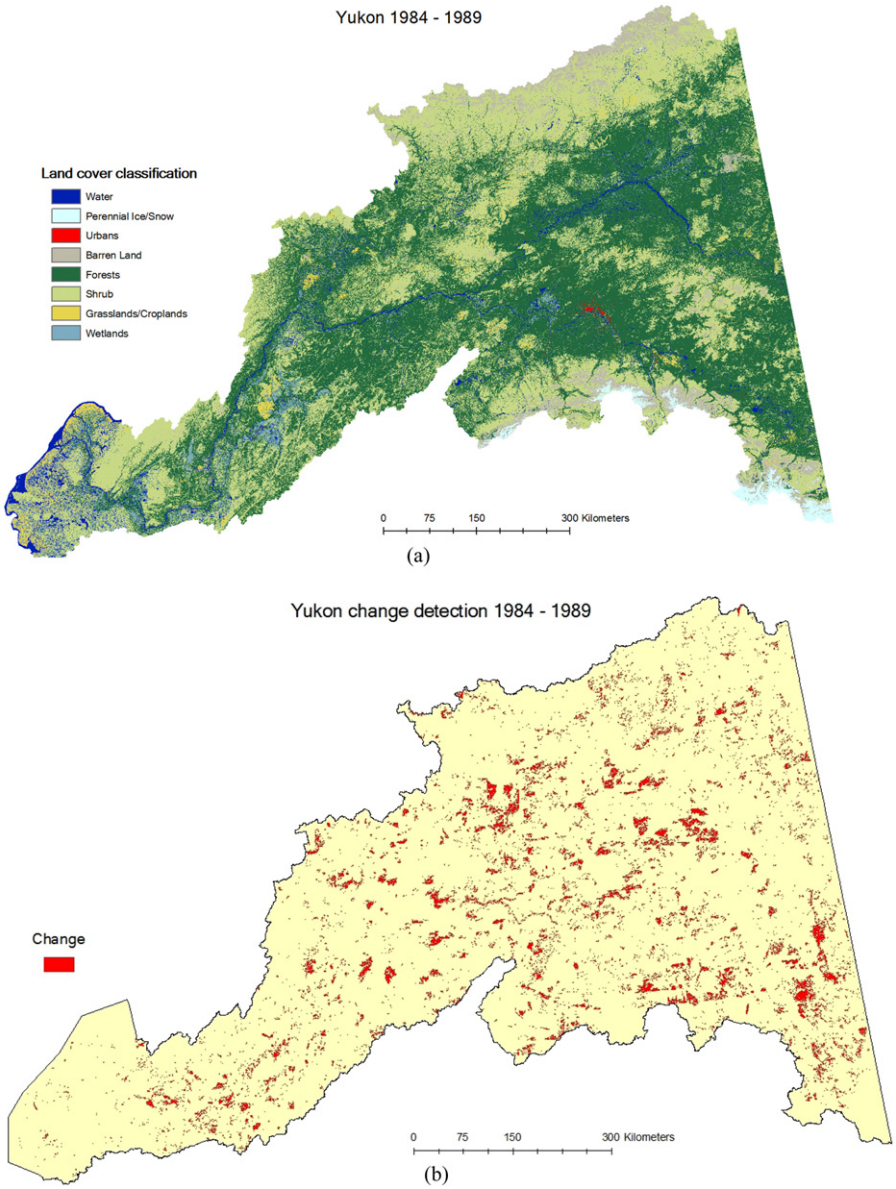

Figure 3. Land cover map (a) and change detection results (b) in the Yukon River Basin for 1984–9. (Continued on next page.)

Table 1. Percentage of land cover types in the Yukon River Basin for different study periods.

	1984–9	1990–5	1996–2001	2001–3 (base)	2003–8
Water	2.826	2.695	2.493	2.41	2.467
Perennial ice/snow	1.189	1.228	1.211	1.20	1.201
Urban	0.082	0.075	0.075	0.077	0.078
Barren land	5.121	5.248	5.139	5.132	5.338
Forests	49.142	49.094	49.125	48.863	48.515
Shrub	37.168	37.242	37.636	38.011	38.009
Grassland/cropland	2.193	2.225	2.128	2.119	2.163
Wetland	2.279	2.191	2.192	2.179	2.228

figure 3 (the maps for the other two periods are not shown). The accuracy assessment is provided in the supplementary material (available at stacks.iop.org/ERL/6/034012/mmedia). The dominant type in the Yukon River Basin is forest, accounting for about 50% of the total area (table 1). The second main type, shrubland, accounts for 37%. Urban regions and perennial ice/snow occupy no more than 1.5%, which are eliminated from the further analysis. Below we analyze changes in the major land cover types and their associated potential causes for our study periods.

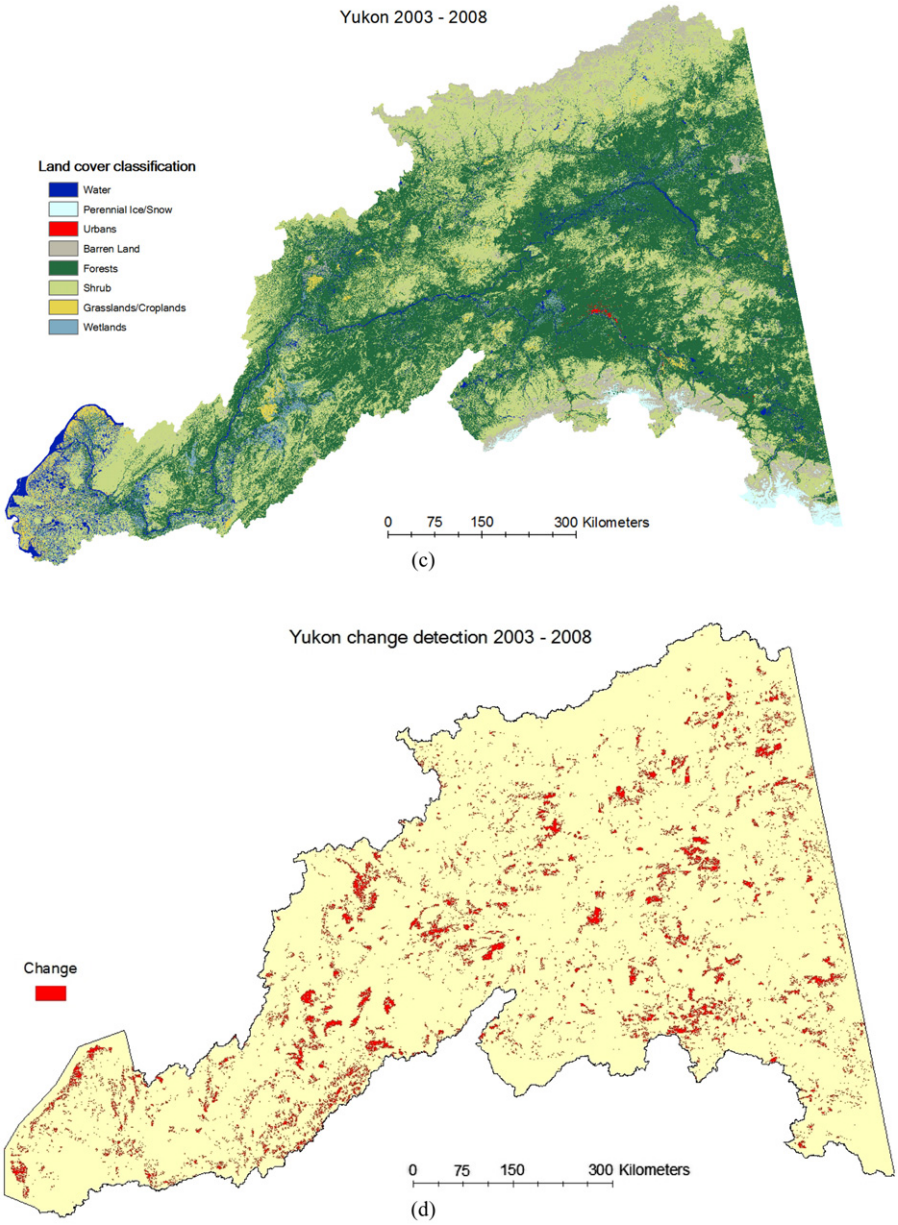

Figure 3. (Continued.) Land cover map (c) and change detection results (d) in the Yukon River Basin for 2003–8.

3.1. Forest area change and wildfire

Percentages of forests including deciduous, evergreen, mixed forest and woody wetlands in 1990–5 and 2003–8 are lower than those in the periods of 1984–9 and 1996–2001, respectively (table 1). Overall, forests declined from the mid-1980s to the present. The decrease is especially obvious comparing 2003–8 with 1996–2001: the percentage of forests decreased by 1% (around 5500 km^2) from the end of the 20th century. There are many patches of disappearing forest area (>5 km^2) between the two study periods of 1996–2001 and 2003–8 (figure 4). The dark patches represent regions with forests during 1996–2001 that were not forest in 2003–8. While climate change may exert some effects on the immense change in such a short time period, we hypothesize that the change was more likely due to fire disturbance. To test the hypothesis, we overlaid the fire burned areas (www.mtbs.gov/dataaccess.html; [29]) in years 2004 and 2005 on the developed land cover maps. We find that wildfire occurrence increased significantly from the period of 1991–2 to 2004–5. Most dark polygons are within the burned regions (the blue circles), especially the high severity areas, although there are some exceptions indicated by the green circles (figure 4). We therefore further examined the two exceptions, which are numbers 1 and 2 in the region (figure 5), where color composite scenes of band5 (red), band4 (green) and band3 (blue) are shown for the two periods. The images during 1996–2001 show a stronger reflectance in the green band and some forests (delineated by white lines) were changed into grassland and shrubland. We searched all the wildfire records (1984–2007) and found no fire occurrence reported for those regions. Thus, we speculate that previously undetected wildfire

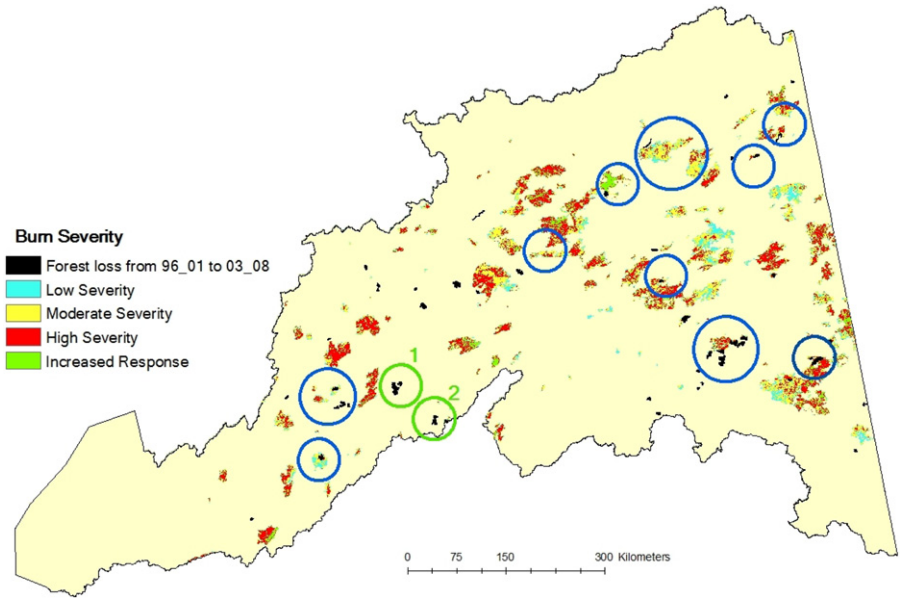

Figure 4. The main patches of disappearing forest (>5 km^2) between two study periods (1996–2001 and 2003–8) and fire history for 2004 and 2005 in the Yukon River Basin. The black polygons represent forest loss regions. More analysis of the loss circled by the two green circles is given in figure 5.

or insect damage might be the most likely causes for the change. Similarly, when we overlay the fire polygons of 1991 and 1992 on the forest disappearing regions between 1984–9 and 1990–5 (not shown here), we find that the wildfire records match the areal change during these periods.

3.2. Change of water bodies

Water surface area decreased by 12.6% from the period 1984–9 to 2003–8 in this region (table 1). The water surface refers to the opened and closed lakes and ponds that lack inlets and outlets, but does not include streams. Since the open water bodies are steadily affected by upstream flows through hydrological networks, we only studied the distribution of the closed water bodies during the study periods. The NHD data, which provide the detailed stream information in the Yukon River Basin, were used to extract the closed water bodies. The lakes and ponds intersected with streams were excluded from further analysis. We also omitted the water bodies whose area was less than 3600 m^2.

Note that the study periods of 1984–9 and 2003–8 have relatively better image quality in terms of cloud fraction and the Sun's elevation angle. Although the cloud removal and terrain correction was carried out, some thin clouds still existed and the effectiveness of the terrain correction was not perfect. As a result, some shadows on images still exist and are wrongly classified as water bodies. Consequently, our analysis of the dynamics of the closed water bodies is only focused on these two periods.

The total number of closed water bodies (larger than 3600 m^2) declined from 168 005 during 1984–9 to 160 965 during 2003–8. The area of the closed water bodies slightly decreased from 764 851 to 764 347 ha during the 25-year period. We conclude that the Yukon River Basin has a general decline in closed water bodies. As expected, the closed water bodies show a smaller change (table 2) in comparison to the dynamics of all water bodies (table 1). Most of the region has permafrost beneath the topsoil. Thus, we incorporated the permafrost distribution [16] into our analysis of the spatial pattern of the closed water bodies' changes. The sporadic permafrost was not considered due to its tiny fraction. The closed water body dynamics varied significantly depending on the different permafrost types (table 2). The general trends are: (1) the closed water bodies increased in both their area and count in continuous permafrost-dominated areas and (2) the closed water bodies underlaid by discontinuous permafrost showed an opposite trend in their count and area in comparison to the continuous permafrost-dominated areas. These results are consistent with a previous study in western Siberia [8]. Fresh water does not infiltrate the continuous permafrost area due to an impermeable layer of permafrost. On the other hand, water above discontinuous permafrost can easily infiltrate the subsurface of the hydrological system. From table 2, we assume that the ice content of permafrost is the fundamental reason for the change of the closed water bodies. Specifically, the closed water bodies in continuous, low ice content permafrost regions may show a similar change trend to those in discontinuous permafrost regions. On the other hand, the closed water bodies in discontinuous, medium ice content permafrost regions could also show dynamical trends like those in the continuous permafrost regions. The key is whether fresh water can find pathways to join the groundwater system. If yes, the closed water bodies shrink; if not, they expand. In the Yukon River Basin, 54% of the area is underlaid by permafrost with high or medium ice content while the rest has low ice content. The increase of the closed water bodies on the former is offset by the decrease of the latter. The growing season (May–September) air temperature in the region persistently

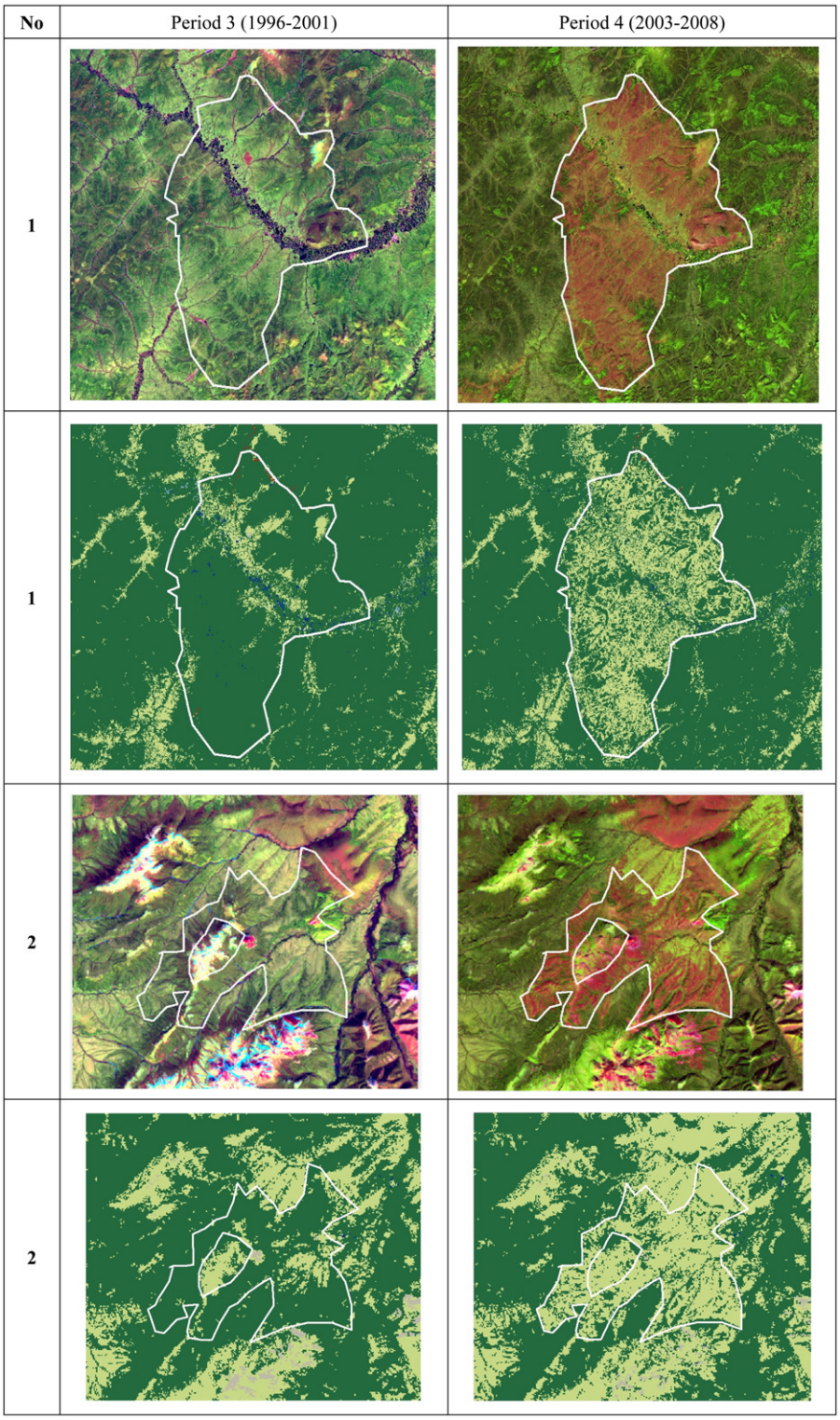

Figure 5. The color composite scenes of band5 (red), band4 (green) and band3 (blue) and land cover maps for the periods of 1996–2001 and 2003–8. The locations of the scenes are indicated by the green circles shown in figure 4.

increased during the study period and permafrost degradation in this region has been reported by a previous study [30], while precipitation fluctuated [23]. Thus, the thawing permafrost very likely plays an important role in the changes of the closed water bodies.

3.3. Changes of shrubland, grassland, and wetland

Shrubland (shrub/scrub and dwarf scrub) increased from 37.2% to 38% from 1984–9 to 2003–8. A large forest area was converted to shrubland (figure 6(a)). Most of the area has

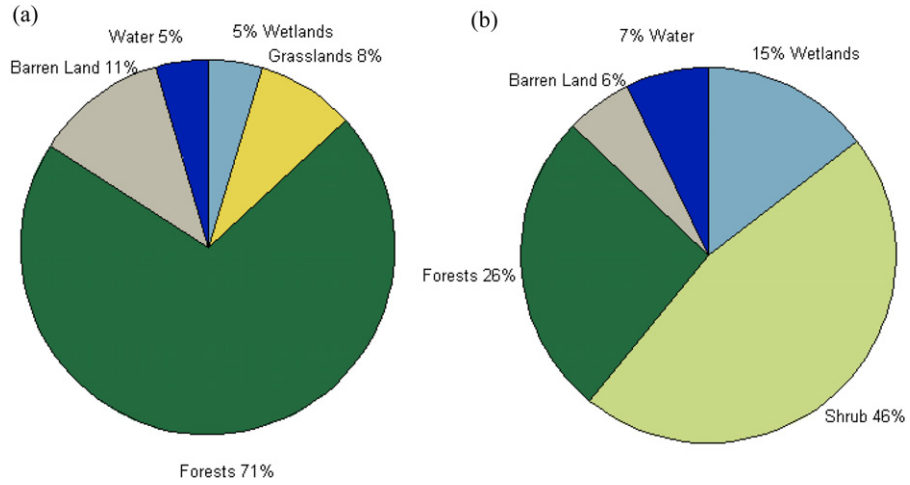

Figure 6. Changes in land cover for specific types in the Yukon River Basin from 1984–9 to 2003–8: (a) proportion of land cover types which were changed to shrub, and (b) proportion of land cover types that grassland/cropland was changed into.

Table 2. Changes of closed water bodies for the four study periods on the different permafrost types. (Only closed water bodies larger than 3600 m^2 are considered; the area unit is ha.)

Change of closed water bodies from 1984–9 to 2003–8		Continuous permafrost				Discontinuous permafrost		
		High ice content (>20%)	Medium ice content (10–20%)	Low ice content (0–10%)	Total on continuous permafrost	Medium ice content (10–20%)	Low ice content (0–10%)	Total on discontinuous permafrost
1984–9	Closed water bodies counts	2190	70 819	7895	80 904	38 066	49 035	87 101
	Closed water bodies area	10 434	407 986	23 846	442 266	120 129	202 456	322 585
1990–5	Closed water bodies counts	2361	74 626	6401	83 388	40 856	38 784	79 640
	Closed water bodies area	11 709	425 920	23 483	461 112	134 125	194 230	328 355
1996–2001	Closed water bodies counts	2415	74 217	5539	82 171	38 870	38 240	77 110
	Closed water bodies area	11 029	429 602	21 001	461 632	128 804	180 267	309 071
2001–3 (base)	Closed water bodies counts	2311	72 952	5456	80 719	37 722	36 234	73 956
	Closed water bodies area	11 205	408 934	21 383	441 522	118 432	163 953	282 385
2003–8	Closed water bodies counts	2393	73 738	5669	81 800	39 349	39 816	79 165
	Closed water bodies area	11 723	417 020	22 472	451 215	130 643	182 489	313 132

fire history, suggesting that forest fire is an important factor in shrub expansion. Meanwhile, some wetlands were drying and succeeded by shrubs and some barren land and grassland was also converted into shrublands.

Grassland/cropland in the Yukon River Basin showed a very small decrease during the 25-year period (table 1). From 1984–9 to 2003–8, some grasslands were invaded by shrub/scrub (figure 6(b)). This is consistent with other studies in this region [12, 31]. Further, about 46% of grassland loss area was taken by shrub/scrub, which might be more likely due to succession. Warming may be another cause. At the same time, some grassland/cropland land covers have been converted into wetlands. We find that 64% of these new wetlands are wetlands that usually have a high variability due to flood events.

Wetland variation showed no consistent pattern (table 2). The areal change of wetlands might be greatly affected by short-term precipitation events. With warming, wetlands could expand in the areas dominated by the permafrost having high or medium ice content where the closed water bodies are increasing. In contrast, wetlands may also shrink due to the decline of the closed water bodies in the low ice content permafrost-dominated areas. Landsat TM or ETM image data are sufficient to separate wetlands from uplands [32], but errors occur in separating wetlands from forests [33]. Thus, wetland changes in the region are subject to further investigation.

4. Summary

The NLCD 2001 data were used as reference information for mapping the land cover change for the four periods from 1984 to 2008. We found that the Yukon River Basin had the following land cover change patterns during the study period: (1) forests were decreasing mainly due to wildfire, (2) the closed water bodies were shrinking possibly due to permafrost degradation if water drains well in discontinuous permafrost regions, (3) shrubs had expanded and also a large portion of grassland was converted into shrubland likely due to forest fire and warming. The results are likely to have a great uncertainty mainly due to acquisition date differences and illumination angles and remaining clouds contamination in the images we used. For instance, the scan line corrector failure on ETM+ made candidate images even less available for the period 2003–8. Consequently, some images with

large acquisition date differences from their reference data were used in order to cover the whole Yukon River Basin in our analysis, which will result in uncertainty. Next, we will use the land cover change data and associated uncertainty information to study the carbon and water dynamics during the last 25 years with biogeochemistry modeling approaches for the region (e.g., [13, 14]).

Acknowledgments

This research is supported by the NSF Arctic System Science Program (NSF-0554811), the NSF Carbon and Water in the Earth Program (NSF-0630319) and the NASA Land Use and Land Cover Change program (NASA-NNX09AI26G). We thank the two anonymous reviewers for providing valuable suggestions on our earlier drafts of this study.

References

[1] IPCC 2001 *Climate Change 2001: The Scientific Basis. Contribution of Working Group I to the Third Assessment Report of the IPCC* ed D Houghton, N Griggs, D Van der Linder and J Maskell (Cambridge: Cambridge University Press)

[2] Hinzman L D 2005 Evidence and implications of recent climate change in northern Alaska and other arctic regions *Clim. Change* **72** 251–98

[3] Hartmann B and Wendler G 2005 The significance of the 1976 Pacific climate shift in the climatology of Alaska *J. Clim.* **18** 4824–39

[4] Serreze M C, Walsh J E, Chapin F S III, Osterkamp T, Dyurgerov M, Romanovsky V, Oechel E, Morison J, Zhang T and Barry R 2000 Observational evidence of recent change in the northern high-latitude environment *Clim. Change* **46** 159–207

[5] Overland J E, Wang M and Bond N A 2002 Recent temperature changes in the western Arctic during spring *J. Clim.* **15** 1702–16

[6] Overland J E, Spillane M C and Soreide N N 2004 Integrated analysis of physical and biological pan-Arctic change *Clim. Change* **63** 291–322

[7] Klein E, Berg E E and Dial R 2005 Wetland drying and succession across the Kenai Peninsula Lowlands, south-central Alaska *Can. J. Forest Res.* **35** 1931–41

[8] Smith L C, Sheng Y, Macdonald G M and Hinzman L D 2005 Disappearing Arctic lakes *Science* **308** 1429

[9] Riordan B, Verbyla D and McGuire A D 2006 Shrinking ponds in subarctic Alaska based on 1950–2002 remotely sensed images *J. Geophys. Res.* **111** G04002

[10] Yoshikawa K and Hinzman L D 2003 Shrinking thermokarst ponds and groundwater dynamics in discontinuous permafrost near council, Alaska *Permafr. Periglac. Process.* **14** 151–60

[11] Stow A D *et al* 2004 Remote sensing of vegetation and land-cover change in Arctic Tundra Ecosystems *Remote Sens. Environ.* **89** 281–308

[12] Tape K, Sturm M and Sracine C 2006 The evidence for shrub expansion in Northern Alaska and the Pan-Arctic *Glob. Change Biol.* **12** 686–702

[13] Zhuang Q *et al* 2003 Carbon cycling in extratropical terrestrial ecosystems of the Northern Hemisphere during the 20th century: a modeling analysis of the influences of soil thermal dynamics *Tellus* B **55** 751–76

[14] Zhuang Q, Melillo J M, Sarofim M C, Kicklighter D W, McGuire A D, Felzer B S, Sokolov A, Prinn R G, Steudler P A and Hu S 2006 CO_2 and CH_4 exchanges between land ecosystems and the atmosphere in northern high latitudes over the 21st century *Geophys. Res. Lett.* **33** L17403

[15] Williams D L, Goward S and Arvidson T 2006 Landsat: yesterday, today, and tomorrow *Photogramm. Eng. Remote Sens.* **72** 1171–8

[16] Brown J, Ferrians O J, Heginbottom J A and Melnikov E S 1998 Circum-Arctic map of permafrost and ground-ice conditions (Boulder, CO: National Snow and Ice Data Center/World Data Center for Glaciology) Digital Media revised February 2001

[17] Homer C, Huang C, Limin Y, Wylie B and Coan M 2004 Development of a 2001 National land cover database for the United States *Photogramm. Eng. Remote Sens.* **70** 829–40

[18] Nielsen A A, Conradsen K and Simpson J J 1998 Multivariate alteration detection (MAD) and MAF post-processing in multispectral, bitemporal image data: new approaches to change detection studies *Remote Sens. Environ.* **64** 1–19

[19] Nielsen A A, Conradsen K and Andersen O B 2002 A change oriented extension of EOF analysis applied to the 1996–1997 AVHRR sea surface temperature data *Phys. Chem. Earth* **27** 1379–86

[20] Canty M J 2007 *Image Analysis, Classification, and Change Detection in Remote Sensing, with Algorithms for ENVI/IDL* (London: Taylor and Francis)

[21] Bishop C M 2006 *Pattern Recognition and Machine Learning* (Berlin: Springer)

[22] Richards J A and Jia X 1999 *Remote Sensing Digital Image Analysis* (Berlin: Springer)

[23] Kistler R, Kalnay E and Collins W 2001 The NCEP-NCAR 50-year reanalysis: monthly means CD-ROM and documentation *Bull. Am. Meteorol. Soc.* **82** 247–267

[24] Toutin T 2002 Three-dimensional topographic mapping with ASTER stereo data in rugged topography *IEEE Trans. Geosci. Remote Sens.* **40** 2241–7

[25] Irish R R, Barker J L, Goward S N and Arvidson T 2006 Characterization of the Landsat-7 ETM automated cloud-cover assessment (ACCA) algorithm *Photogramm. Eng. Remote Sens.* **72** 1179–88

[26] Simpson J J and Stitt J R 1998 A procedure for the detection and removal of cloud shadow from AVHRR data over land *IEEE Trans. Geosci. Remote Sens.* **36** 880–97

[27] Teillet P M, Guindon B and Goodenough D G 1982 On the slope-aspect correction of multispectral scanner data *Can. J. Remote Sens.* **8** 84–106

[28] Chander G, Markham B L and Helder D L 2009 Summary of current radiometric calibration coefficients for Landsat MSS, TM, ETM+, and EO-1 ALI sensors *Remote Sens. Environ.* **113** 893–903

[29] Epting J, Verbyla D and Sorbel B 2005 Evaluation of remotely sensed indices for assessing burn severity in interior Alaska using Landsat TM and ETM+ *Remote Sens. Environ.* **96** 328–39

[30] Jorgenson M T, Shur Y L and Pullman E R 2006 Abrupt increase in permafrost degradation in Arctic Alaska *Geophys. Res. Lett.* **33** L02503

[31] Sturm M, Sracine C and Tape K 2001 Increasing shrub abundance in the Arctic *Nature* **411** 546–7

[32] Wright C and Gallant A 2007 Improved wetland remote sensing in Yellowstone National Park using classification trees to combine TM imagery and ancillary environmental data *Remote Sens. Environ.* **107** 582–605

[33] Ozesmi S L and Bauer M E 2002 Satellite remote sensing of wetlands *Wetlands Ecol. Manag.* **10** 381–402